JOURNAL OF GEOPHYSICAL RESEARCH, VOL. 102, NO. B4, PAGES 8381–8396, APRIL 10, 1997

Temporal variations of the coda decay rate on Kamchatka: Are they real and precursory?

A. A. Gusev

Institute of Volcanic Geology and Geochemistry, Russian Academy of Science, Petropavlovsk-Kamchatsky
Instituto de Geofisica, Universidad Nacional Autónoma de México, Mexico City, Mexico

Abstract. Temporal variations of the decay rate of the coda of local earthquakes are studied for four Kamchatka stations. To suppress any bias caused by the coda Q versus lapse time dependence, I use the deviation of an individual coda decay function from the empirical reference decay function, and the analysis is done over a fixed lapse time window. For each individual coda record, a decay rate parameter "α" is determined by the following procedure. First, the reference log coda decay function is subtracted from an individual one giving a residual function; second, the slope of this residual versus lapse time is determined over the fixed lapse time window giving an α estimate. The data used are records of 150-250 Kamchatka earthquakes of 1967-1990 (M_L=3.5-5) obtained by four stations employing three-component 1-s seismographs. The processed data show apparent temporal variation of α with high statistical significance. Several possibilities are then investigated of mimicking the genuine temporal variation of α by systematic variation of other parameters, first of all epicenter wandering and nodal plane rotation. This analysis does not reveal any strong bias and thus suggests that the observed variation is genuine. Then I show the significance of five apparently precursory anomalies identified retroactively. Also, I describe briefly the real-time prediction experiment conducted on Kamchatka for 1982-1990 using coda decay, aimed at the intermediate-term forecasting of large Benioff zone earthquakes. This experiment resulted in the successful forecast of the August 17, 1983, M_w=7.0 event with an accuracy of 2 months in time and 100-200 km in location; magnitude was overestimated by 0.5. Later, a false alarm was also issued. Thus the experiment confirms the reality of the coda decay rate precursor but also shows that it needs further improvement to become reliable. Physically, the variations of the coda decay rate are associated with time-dependent local variations of scatterer density in the lithosphere.

Introduction

The well-known relative stability of the coda envelope shape [*Aki*, 1969; *Aki and Chouet*, 1975; *Rautian and Khalturin*, 1978], which is believed to reflect the coda formation mechanism as random (back)scattered waves, provides a reasonable basis for the detection of possible temporal variations of absorptive or scattering properties of the lithosphere. With single-station data, this can be done most easily employing the coda decay rate [*Chouet* 1979; *Gusev and Lemzikov* 1980, 1984, 1985]. *Aki* [1985] interpreted possible precursory coda decay rate variations in terms of variations of S wave Q factor ("coda Q"); *Jin and Aki* [1986] have shown how this technique works with real data. The first wave of such studies, addressed mainly at temporal variations of precursory value, was summarized by *Sato* [1988] wherein additional references can be found. In response to the suggestion of the International Association of Seismology and Physics of the Earth's Interior subcommission on earthquake prediction, *Jin and Aki* [1990] and Sato (using the [*Sato* 1988] paper as an application document) proposed that the coda-Q technique be formally evaluated as an earthquake precursor. These materials are included in the relevant publication [*Wyss*, 1991], and followed by ample discussion, of which the aim was to find out whether the use of coda decay rate anomalies can indeed be considered as a valid step to prediction technology. The response of the evaluation panel revealed wide doubts regarding the mere existence of any genuine variation, be it precursory or not. One of the motives of such a response was the introduction of an improved technique of coda monitoring based on small earthquake doublets [*Got et al.*, 1990; *Got and Frechet* 1993; *Beroza et al.*, 1995; *Hellweg et al.*, 1995]. This high-resolution technique has demonstrated (for coda lapse time typically below 30 s) the general lack of substantial temporal variation in general and of precursory variation in particular, as well as the high susceptibility of coda envelope shape to nodal plane, source directivity, or depth variations. An equally pessimistic conclusion was reached by *Aptikaeva and Kopnichev* [1993]: in their more traditional but very detailed study they found examples of high susceptibility of early coda shape to source location, well capable of imitating temporal variations if the source hypocenter would wander.

The set of criteria and critical comments given by *Wyss* [1991, pp. 46-55] by the members of the review/evaluation

Paper number 96JB03490.
0148-0227/97/96JB-03490$09.00

team, aimed at verifying the genuine temporal variation, seems somewhat too exacting and not fully congruent, but as a whole it presents a good starting point for such a verification. One can summarize possible causes of fictitious temporal variations [after *Wyss* 1991, pp. 46-55] as follows: (1) purely random fluctuations of low statistical significance; (2a) (systematic) spatial (epicenter and/or depth) variation of the coda decay rate in combination with hypocenter wandering over the data selection volume; (2b) (systematic) generation of slow-propagating (guided) waves contaminating "normal" coda for some hypocentral locations (specific version of 2a); (3a) (systematic) variation of average magnitude; (3b) (systematic) source spectrum variations (this is the real underpinning of 3a); (4) (systematic) nodal plane variation; (5) oversampling of some spatial volume - nodal plane combinations due to swarms; and (6) effect of varying angles of incidence (not important for late coda).

Many of these points had already been discussed by *Gusev and Lemzikov* [1980, 1984, 1985] and *Sato* [1988]. They also had mentioned: (2c) (systematic) *T* phase contamination (a specific version of 2a); (7) instrument parameter drift, miscalibration; (8) (systematic) human error (for manual or interactive processing modes). On the basis of the work of *Got and Frechet* [1993], one can also add (9) (systematic) source directivity variations.

It should be mentioned that in many cases, the reviewers [*Wyss,* 1991, pp. 46-55] did not fully acknowledge that, while the possibility indeed exists that the dependence of coda decay on any "interfering" parameter involved can mimic temporal variation, this is no more than a possibility. Simple scatter in any interfering parameter merely increases the data noise, so that exclusively systematic, i.e., correlated with time, variations of the listed parameters are capable of producing fictitious temporal anomalies. This kind of logic was the basis of a test employed by *Gusev and Lemzikov* [1980, 1984, 1985] to check the reality of temporal variations claimed to exist in these papers. They plotted the spatial distribution of epicenters for two periods, "normal" and "anomalous," with clearly different average values of the coda decay rate, and found that both distributions were visually similar, with no expressed wandering of an "average epicenter." In the following I apply a more efficient technique that may substantially suppress spurious effects of gradual spatial variation of coda parameters.

The present study is based on the Kamchatka coda decay rate data for a 24-year observation period. Temporal variations of the coda decay rate are obvious in Kamchatkan data. Hence my first aim is to find out whether these variations are genuine, or only apparent, being produced by one of the listed interfering factors. I use data of two out of the three stations already reported by *Gusev and Lemzikov* [1980, 1984, 1985] to show precursory coda decay anomalies on Kamchatka. For the third station, situated on Bering Island, there is the convincing evidence of the *T* phase contamination of coda. Although I do not believe this contamination to be the real source of the anomaly reported for this station (data with strong *T* phase effects have been screened out), I excluded it from the present study because it is difficult to screen out weak to moderate T phase effects. Data from two more stations are added, the time span is increased from 10 to 24 years, and the data processing technique is improved.

My second aim is to investigate the reality of precursory coda decay rate anomalies. For 1967-1981 I analyze such anomalies based on retroactively processed data. In 1982-1990, however, coda decay data were processed and analyzed in the course of the real-time prediction experiment. Some results of this practical check of the first version of the coda precursor methodology are given below as well.

Coda Decay, Measurement of Its Rate, and Possible Biases

Data of four stations (KBG, KRI, SPN, and PET) of the regional Kamchatka network (Figure 1) were chosen for the detailed study. The network employs three-component galvanometric registration using 1.2-s pendulums of VEGIK or SM-3 type, with GB-IV type galvanometers of 0.07-s period. The instrument response (of identical ($\pm$10-15%) shape for all stations and components) is practically flat to displacement between 1 and 10 Hz. The magnification value is in the range 3-10,000. The visual frequency (measured as half a number of peaks and troughs over a 50-s window) of coda waves recorded by these instruments is well defined and varies only slightly over the network; its typical values are 1.2-1.6 Hz at the lapse time $t=75\pm25$ s, 0.9-1.2 Hz at $t=150\pm25$ s, and 0.75-1.1 Hz at $t=250\pm25$ s (lapse time here and throughout the paper is always measured from the origin time t_o). All these estimates correspond to the magnitude range studied below, and they are rather stable within this range. The relatively narrowband character of a coda record probably reflects the combined effect of a medium attenuation filter and of the abrupt (f^3) lower cutoff of the instrument response. A complete calibration routine for these instruments was repeated once a year. In addition, each 8-hour three-component photorecord includes, on each component, a test signal generated by a stable-amplitude sweep-frequency generator forcing the calibration coil. This test signal provides the permanent control on the gross transfer function stability.

A segment of the tail part of a record of a near earthquake, between the moment (origin time + 1.7 (*S* wave travel time)) or later, and the moment when the trace amplitude becomes twice as large as the microseisms (if such a segment is not shorter than 70 s) was considered as the "coda window" within which the amplitude measurements were made. A coda window is then subdivided into successive 10-s segments. Segment boundaries are fixed and "rounded off" in terms of lapse time, that is, they are set at the moments of the lapse time $t_i=10i=40$, 50, 60 ... where $i=4$, 5, 6, ... Then the value of peak-to-peak amplitude $2A_i$ of the most prominent excursions is measured in the 10-s segments on each component. The result is then ascribed to the center of the interval, that is, to the lapse time moment of 45, 55, ... s. A sequence of no less than seven successive $2A_i$ values specifies each processed component. Practically, the earliest measured interval was often later than 40-50 s. Figure 2 shows an example of a three-component record. The photographic paper used is intentionally low contrast and thus somewhat difficult to reproduce; however, at the employed fast paper speed of 2 mm/s, codas, if not off scale, are fully legible.

In order to analyze coda decay rate variations in a meaningful way, one must get rid of the possible bias produced

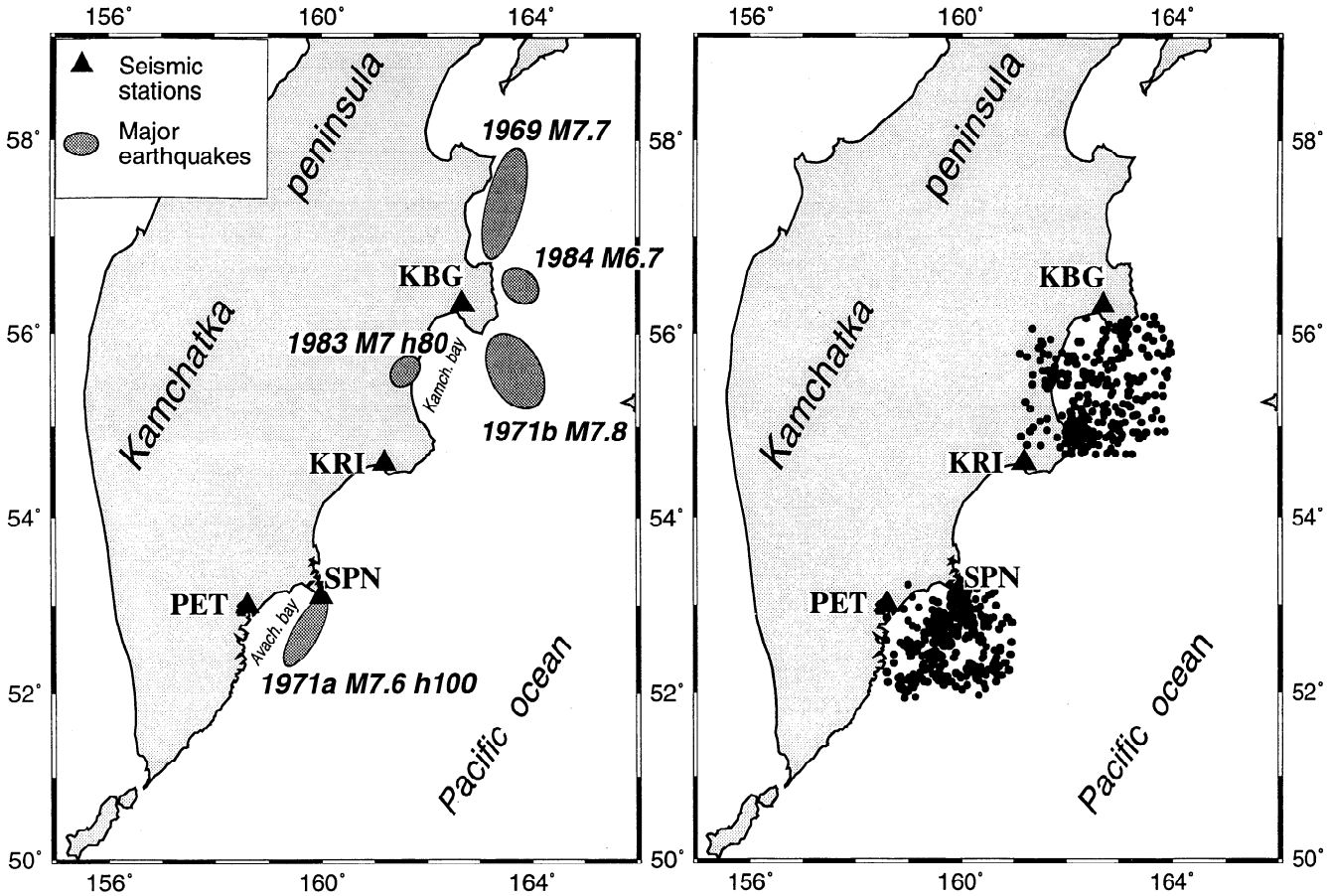

Figure 1. The region of the study. (left) Seismic stations, data of which were used, and major earthquakes. (right) Two epicenter clusters show earthquakes of 1967-1990 used with each station pair: KRI and KBG with the northern cluster; PET and SPN with the southern cluster.

by the dependence of the mean coda decay rate ($d \log A/dt$) on the lapse time. This can be attained in two ways: one can measure residual decay variations after subtracting from data the average (reference) empirical coda shape with its lapse time dependent decay rate, as proposed by *Gusev and Lemzikov* [1980, 1984, 1985], and/or one can use a rigidly fixed lapse time subwindow [*Hellweg et al.*, 1995]. My experience shows that the first technique is rather efficient. However, it was qualified here as not sufficiently rigorous for the aims of the present study and was thus combined with the second. The following equation gives the definition of the coda decay parameter α [*Gusev and Lemzikov*, 1980]:

$$\alpha = -\frac{d}{dt}[\log 2A(t) - \log a(t)] \quad (1)$$

where $a(t)$ is the reference coda shape function. It is the basis for the regression equation used in actual data processing:

$$\alpha t_i + \beta = \log 2A_i - \log a(t_i). \quad (2)$$

where $i = i_1, i_1+1, \ldots, i_2$, and the pair (i_1, i_2) is fixed rigidly.. To use equation 2 one needs the estimate of $a(t)$. *Gusev and Lemzikov* [1980] determined such an empirical average coda shape function $a(t)$ for Kamchatkan stations; it is judged to be sufficiently accurate and is used below without further correction. Figure 3 shows the measured coda decay for two example earthquake records - "normal" and "anomalous", and the reference $a(t)$ curve.

For the described approach to be intrinsically consistent, the reference/average shape must be stable and independent of such possible distorting factors as station, component, epicentral location, depth, and magnitude. Let us consider the difference between the reference and some particular coda shape as a function of lapse time and expand it into the Taylor series. In a study aimed at α variations, only the stability of the linear term of this expansion is relevant; this merely means that the average α value must be zero for any data subgroup. This was thoroughly checked by *Lemzikov and Gusev* [1989], and the results of this study have been summarized by *Gusev* [1995a], so that only the key points will be repeated here. Estimates of α were determined for many earthquakes grouped by source depth, station, and magnitude, for two time periods. Almost for all data groups, and for all in the depth ranges of 0-60 and 60-120 km, the average α values were in the range $\pm 0.6 \times 10^{-3}$ s^{-1}, and the estimated rms errors of these averages were of the same order: 0.5-1 $\times 10^{-3}$ s^{-1}; hence the average α for any subgroup was insignificantly different from zero. Also, α was found to be independent of the choice of an instrument component. A check for the epicentral region dependence

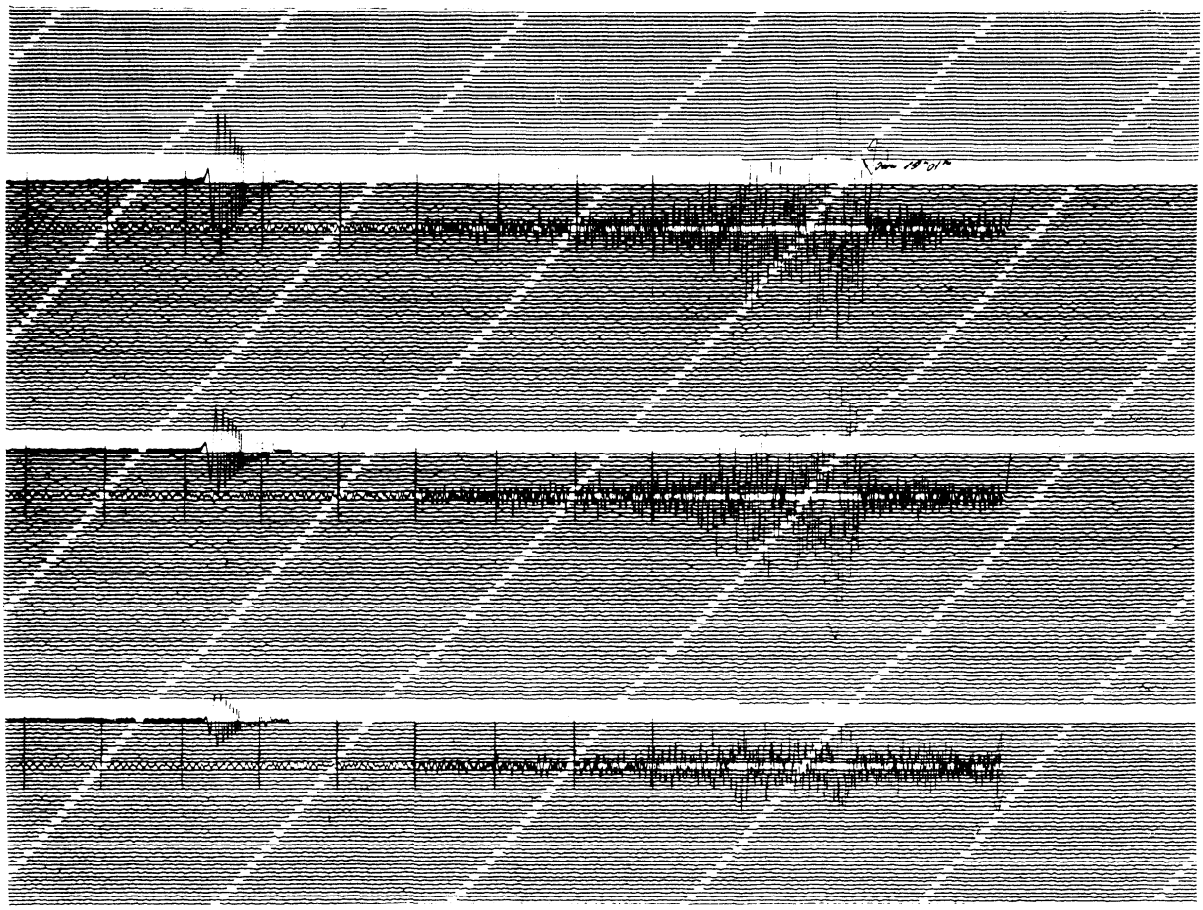

Figure 2. An example seismogram of the station PET. Three components are (top to bottom) E-W, N-S, and Z. Note sweep-frequency test signal in the beginning of the record. Vertical dashes (each 10 s) are pencil marks separating coda subsegments used for coda amplitude measurement; they are synchronous on all records with respect to the origin time of an event (see text).

was not included, however, in the program of any previous study.

The possible magnitude dependence of α must be discussed in more detail. One can expect an effect of this kind to be produced by the probable systematic increase of coda average frequency (and, thus, the degree of attenuation) with decreasing magnitude. This effect does exist. The value of α equals 0 for $m_b \approx 4$-6 is about -1×10^{-3} s^{-1} at $m_b \approx 3.3$ and about -2.5×10^{-3} s^{-1} at $m_b \approx 2.9$. (A. A. Gusev and V. K. Lemzikov, unpublished manuscript, 1984). Thus the magnitude dependence happens to be substantial only for magnitudes below some definite critical value, equivalent to $m_b \approx 3.7$ [*Gusev and Lemzikov*, 1980, 1984, 1985]. This critical value is used below to set the lower magnitude threshold for the data selection.

In this paper I do not study variations of source spectra as a probable source of α instability. However, such a check has been implicitly made for a subset of the present data set,

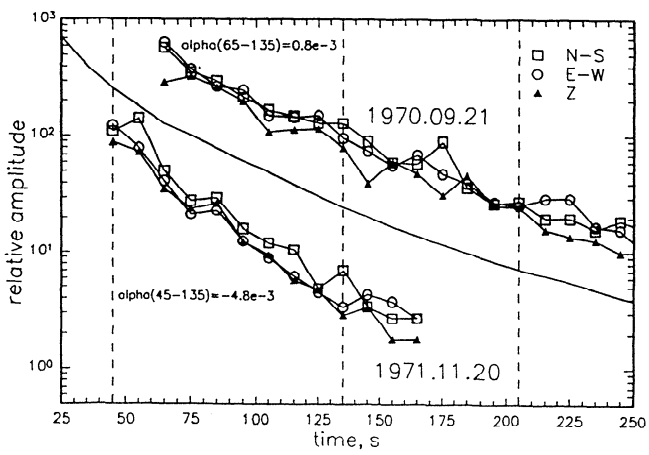

Figure 3. The average coda decay function (smooth curve) and the measured coda peak-to-peak amplitudes in successive 10-s intervals for each of the three components, for two earthquakes. The upper bunch of three curves corresponds to a "normal" event, with coda decay shape near the average one. The lower bunch is for an "anomalous" event, with the coda decay evidently steeper than the average. Note its origin time, a month before the $M=7.9$ event of December 15, 1971. Vertical dashed lines indicate the boundaries of two fixed lapse time windows used for α determination. Also, α values, averaged over all components, are given for each event for the earlier window. The difference between the two α values is 5.6×10^{-3}, or 2.9σ (see Table 5 for σ values). The amplitude curves are shifted arbitrarily along the ordinate axis for clarity of graphical presentation.

studied by *Gusev and Lemzikov* [1984, 1985], with respect to the prominent negative α anomaly of 1971 at KBG. It was shown that at this station, the yearly average frequency of coda (averaged over the individual values measured as indicated above) was at its minimum in 1971, probably reflecting the variations of average source spectra. Usually, the lower the source characteristic frequency, the lower the attenuation; so one could expect flatter/longer codas and a positive α anomaly in this year. The actual anomaly had the opposite sign. Thus source spectral variations do not seem to cause a significant α instability and, thus, considerable fictitious temporal anomalies.

The instrument calibration errors and their possible effect on the stability of α estimates was discussed at some length by *Gusev and Lemzikov* [1980, 1984, 1985] and *Gusev* [1995a]; from this discussion one can conclude that this effect cannot be large. Note that errors in the value of magnification are irrelevant to the estimation of α and that a significant drift of the pendulum period would reveal itself as an apparent spectral change manifested as the change of visual frequency of a record. Such changes were studied systematically by *Gusev and Lemzikov* [1980, 1984, 1985], who did not find any remarkable variation. The only exclusion is the anomaly of 1971 on KBG, described in the preceding paragraph. It was observed over all three components of the station and thus hardly can be ascribed to the instrument drift. Also, correlation of α anomalies over the three channels of a station and over a pair of adjacent stations practically excludes the instrumental origin of variations.

Data Selection and Processing and Epicentral Correction

One can see from Figure 1 that within each pair of selected stations (KBG-KRI and SPN-PET), the stations are at no more than 150-km distance. True coda anomalies, related to variations of properties of the lithosphere, can be expected to show themselves on both adjacent stations. To minimize spurious variations, a compact common epicenter selection area was chosen for each pair. The areas are shaped partly by setting the upper limit to the hypocentral distance. This is needed to measure the coda amplitudes sufficiently early: *S-P* must be below 17 s for the coda window to start at 40 s. Actual epicentral distributions for each station are shown in Figure 1. The magnitude selection interval was K_s=9.6-12.5, that corresponds approximately to $m_b \approx$3.7-5.2 or

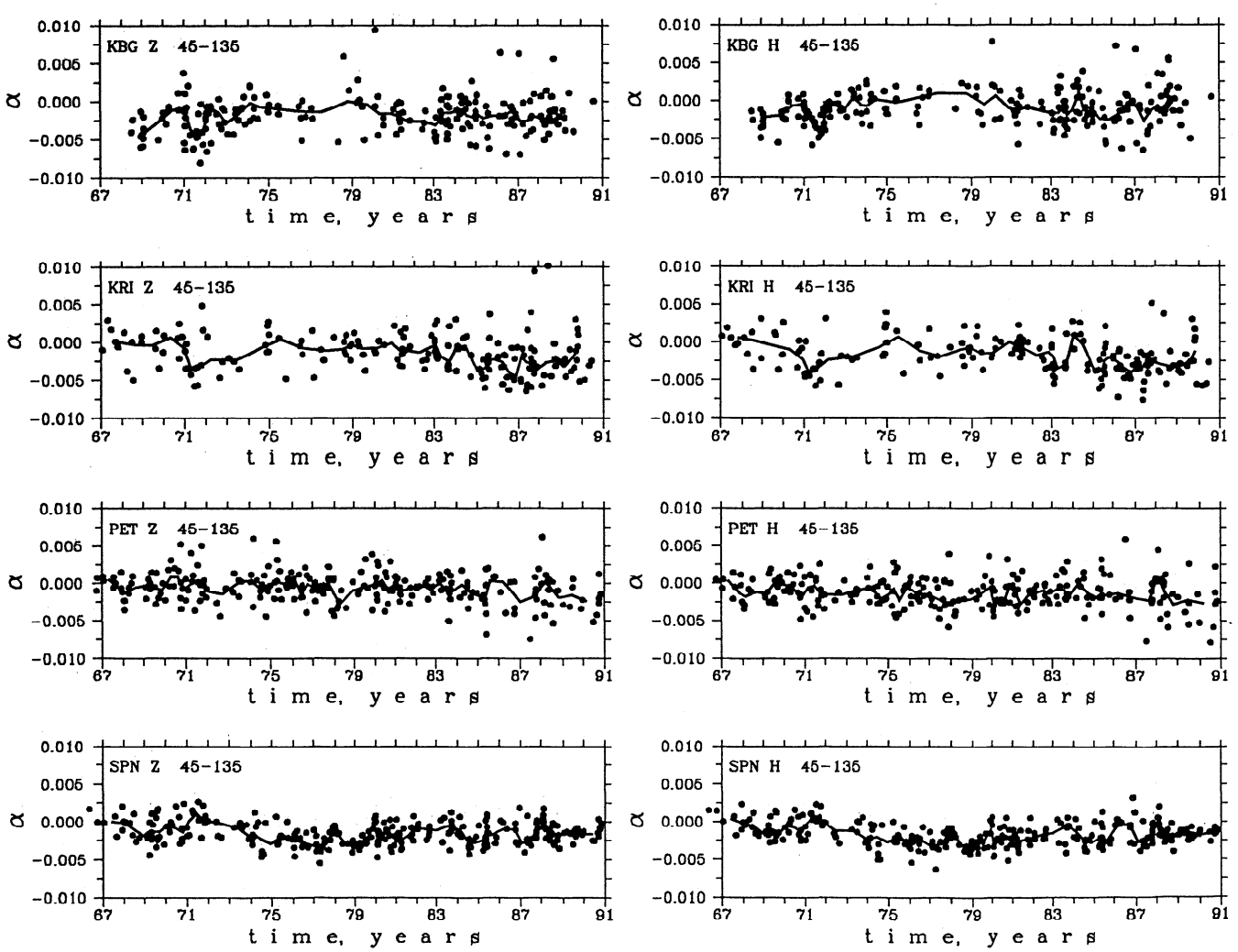

Figure 4. Individual uncorrected α values for 45- to 135-s window, versus event time. (left) Four stations, Z components; (right) same, "H" components. The lines connect medians of successive eight-point groups.

$M_L \approx 3.9$-5.4. (K_s, or merely K, is regional magnitude of the Russian "energy class" type, the only one in the catalog used.) The depth selection interval was 0-100 km. The time period analyzed here begins in 1967 for SPN, PET, and KRI and in 1968 for KBG, when this station was installed. The last analyzed year is 1990. Events in dense swarms were intentionally decimated in order to not give an excessive weight to the data from a narrow location. The two particular fixed lapse time windows used were 45-135 s and 135-205 s. A data set for a single window must therefore contain 10 and 9 data points, respectively. Actually, the measurements with as low as 8 or 7 data points, respectively, were included into the data set; e.g., the data for the particular windows of 45-115 s or 65-135 s were still included into the 45- to 135-s data set.

The general view of the processed $\alpha(t)$ data (45- to 135-s window) is seen in Figure 4 (see Table 1 for details). Throughout the paper, along with the vertical (Z) component data, I use α values averaged over two horizontal components; these data are denoted as the "H" component. The lines on this and the subsequent plots show running eight-point medians with 50% overlapping (jumping by four points). One can note a marked correlation between the components and an apparent temporal variation. The coefficients of correlation between the series of single-event α values for two components of a station are almost always in the range 0.65-0.75.

As explained above, a possible systematic bias of α values related to the epicenter, depth, and magnitude variation may produce fictitious α anomalies. Of these parameters, only the effects of depth h and magnitude K were examined earlier [*Gusev and Lemzikov*, 1980, 1984, 1985]; these were found negligible. To make an additional check, I show here the $\alpha(h)$ and $\alpha(K)$ distributions (Figure 5). A parabolic least squares fit is shown as well. One can see no linear trend for $\alpha(K)$ and a very slight trend for $\alpha(h)$. Also, any systematic temporal trend is absent in K or h values; this means that even if the dependence of α on K or h were real, it would not be able to produce fictitious α anomalies. Figure 5 shows the data for the KBG-KRI pair; for the SPN-PET pair, the results are similar. Thus magnitude and depth can be excluded with certainty as a source of apparent temporal anomalies.

Table 1. Values of the Fisher F Statistic Used to Demonstrate Reality of Temporal Variations of α

Station and Component	N	F	m	n	$F_{m,n,99\%}$[a]	$F_{m,n,99.9\%}$[a]
		45- to 135-s Window				
KBG Z	204	2.50[b]	16	187	2.09	2.75
KBG H		3.00[c]				
KRI Z	180	3.53[c]	14	165	2.18	2.80
KRI H		3.29[c]				
PET Z	240	1.11	19	220	1.96	2.60
PET H		0.94				
SPN Z	276	1.62	22	253	1.92	2.50
SPN H		5.29[c]				
		135- to 205-s Window				
KBG Z	84	0.61	6	77	3.05	4.20
KBG H		1.29				
KRI Z	48	2.10	3	44	4.26	6.55
KRI H		4.88[b]				
PET Z	84	0.64	6	77	3.05	4.20
PET H		1.22				
SPN Z	72	1.07	5	66	3.31	4.80
SPN H		0.31				

[a]Critical Values of F Distribution
[b]Significant deviations for 1% level.
[c]Significant deviations for 0.1% level.

With the epicenter-related anomalies the situation is different. Figure 6 shows smoothed α values as relief maps. The smoothing/averaging technique used is the weighted averaging of the data from the 40 nearest epicenters, with the relative weights equal to inverse-squared epicentral distances. Marked spatial variations are seen. To suppress this source of a fictitious temporal variation, I used the maps of Figure 6 as the epicenter-dependent corrections. The thus corrected α versus time curves are shown in Figure 7 together with the "raw" ones. The error bars ($\pm 1\sigma$) show the rms errors estimated for each eight-point group average through the inter-quartile width. The most evident visual difference between the corrected and the raw data is the constant shift. It is caused by a slight deviation of the true average coda shape for a particular station/component from the accepted network-averaged

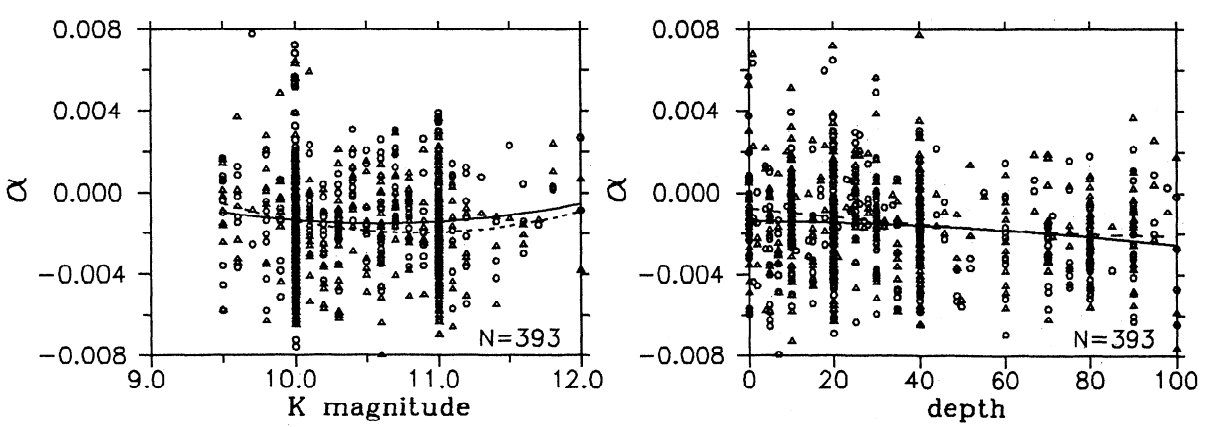

Figure 5. (left) "K" magnitude versus α and (right) depth versus α. Triangles and circles are individual α values (45- to 135-s window) for Z and H components, respectively; solid (Z) and dashed (H) lines show parabolic regression of these data. Data of stations KBG and KRI combined.

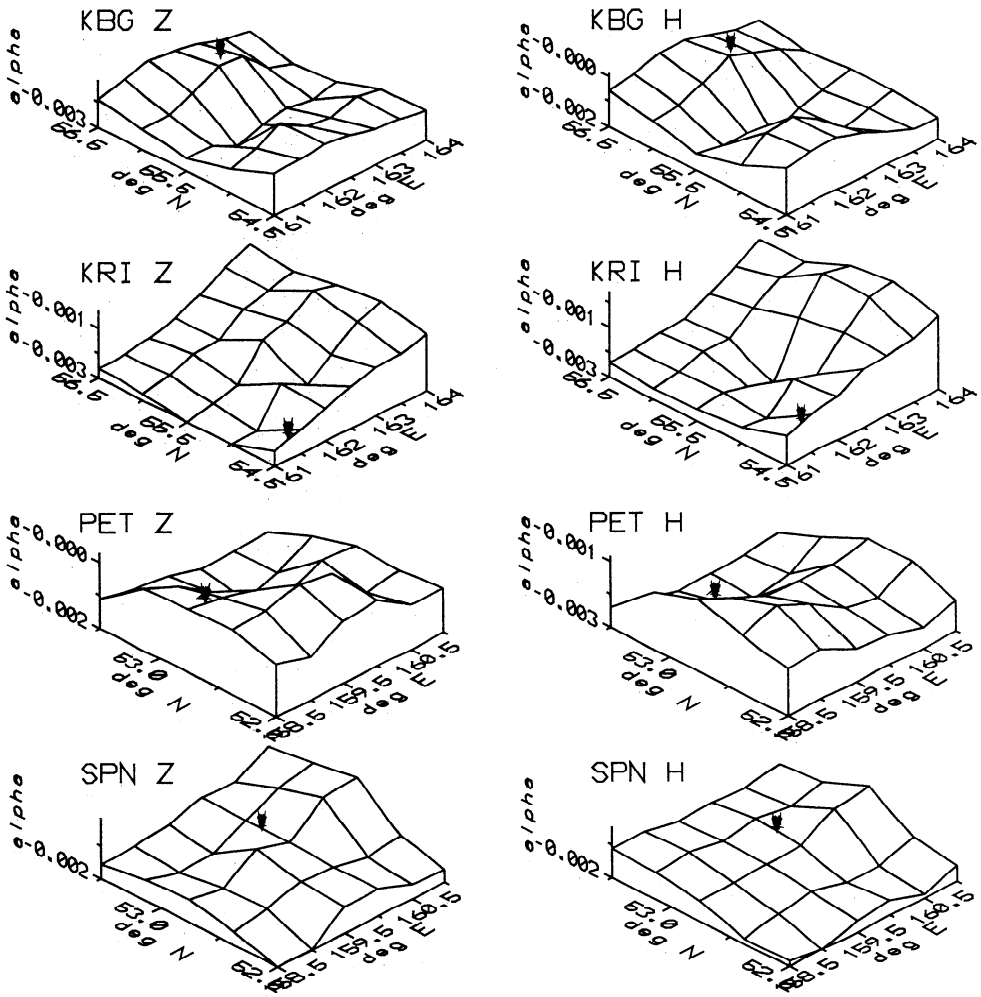

Figure 6. Relief maps of smoothed α values in a perspective view, seen from the southwest. (left) For Z components of the four stations; (right) same, for H components. Both upper and lower group of four graphs uses a common geographic grid and a common vertical scale. Each grid α value is the weighted average of the nearest 40 data points (see Figure 1), with the weight decreasing with epicentral distance as $1/(\text{distance})^2$. The vertical arrowhead on each graph indicates the location of the station whose data are shown.

reference shape. The epicentral corrections incorporate this constant shift, thus making the average level of the corrected data approximately zero. This shift has nothing to do with the temporal variation. The constant shift aside, the corrections produce only minor changes for KBG and KRI and almost no change for SPN and PET. The corrected average lines for KBG and KRI do show somewhat decreased amplitudes of apparent temporal anomalies, but this decrease is marginal. One can ask why the epicentral effect is so clear as such and so inefficient as a cause of a fictitious temporal variation. The answer is that epicentral distribution in the Benioff zone is rather stable, and any significant "epicentral wandering" (that is, systematic drift of average epicenter) is unusual. Informal checks of such a wandering has been already included in the prior publications [*Gusev and Lemzikov*, 1980, 1984, 1985] as mentioned above.

I applied the same epicentral-correction procedure to the α data for the 135- to 205-s coda window. The data volume is smaller because only the larger events can produce coda that is sufficiently long to allow measurements. Figure 8 shows the raw data. In this case, the epicentral corrections were minor, but I applied them in a similar way for uniformity. Figure 9 shows the group-averaged corrected data with the error bars. Here the temporal variations are much weaker as compared to those for the earlier coda window. This difference suggests that the formation of variations by human measurement inaccuracies or instrument drift is improbable, because the measurement procedure and the instruments were identical for both windows.

Statistical Verification of Reality of the Temporal Variations

Before any discussion of the precursory meaning of the temporal coda variations, one must show that some genuine temporal variations exist at all. To do this, one must reformulate the problem of existence as a statistical one. It is clear a priori that the character of the data precludes the verification of short-term anomalies, with the durations

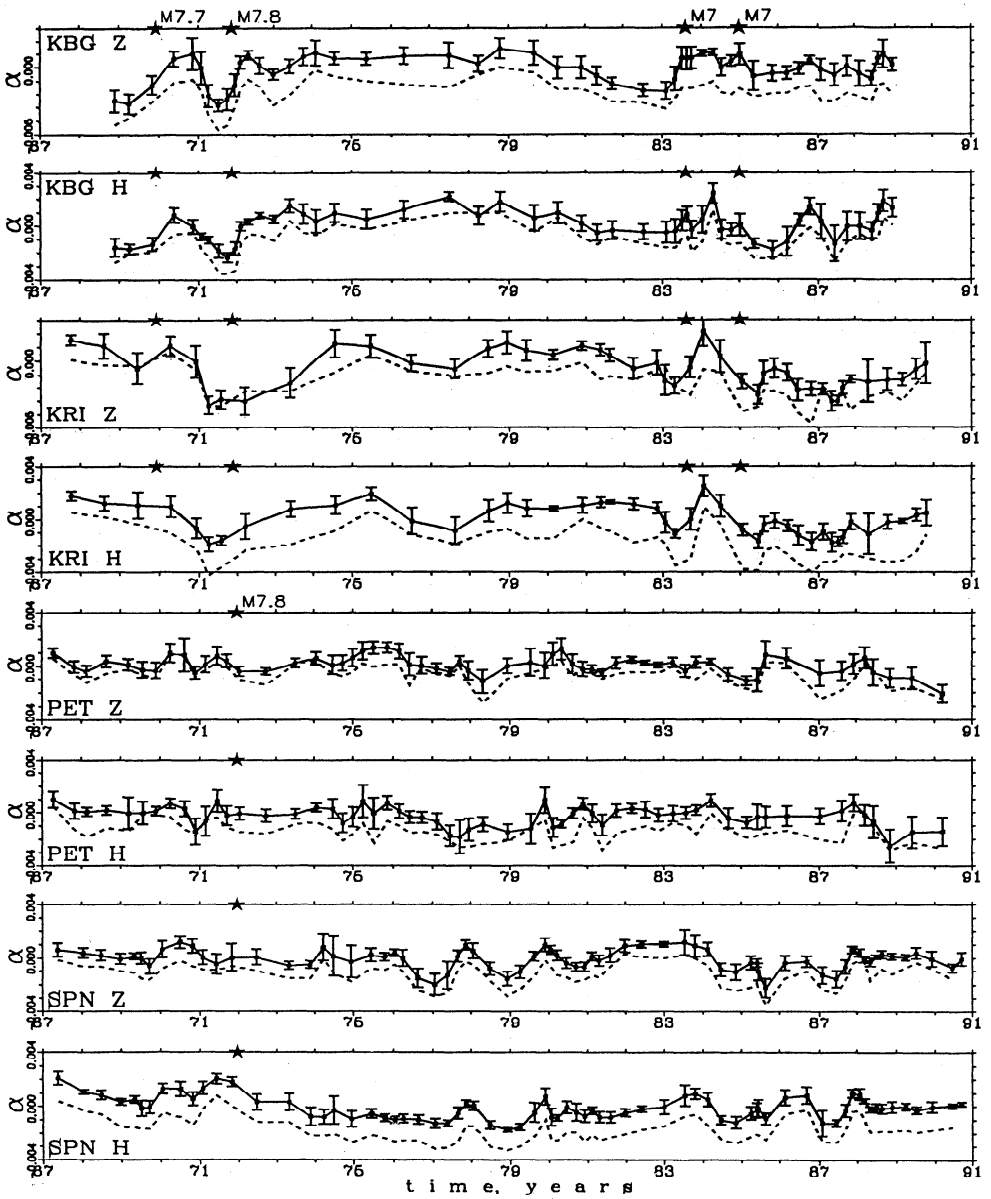

Figure 7. Smoothed epicenter-corrected α versus time data (45- to 135-s window). Four groups of two graphs are shown, one group for each station. Each group consists of a graph for the Z component (upper graph) and that for the H component (lowergraph). The running averages by eight-point groups are shown for the corrected data (solid line) and, for comparison, for the "raw" data (dashes). For the corrected data, error bars ($\pm 1\sigma$) are given showing rms error of an eight-point group average; they are based on the value of interquartile width within each group. Stars on this and further plots mark the moments of major earthquakes in the vicinity of each station (compare Figure 1).

comparable to an interevent time, because such anomalies cannot be distinguished from the data scatter. Hence I confine my study to the variations that are of sufficiently long duration to show themselves in the grouped data. To demonstrate the presence of this kind of variation, I apply the standard analysis of variance (ANOVA) and compare the within-group and intergroup variances. If a temporal variation of sufficiently large amplitude and of appropriate period (comparable to the duration of a group) is present, it will manifest itself as a relative increase of intergroup variance; the significance of such an increase can be tested by means of the Fisher F statistic. In planning an analysis of this kind, one cannot choose a group size that is too small because the noise suppression by averaging will be insufficient; on the other hand, using groups that are too large may suppress all variations but very long-period ones. In the analysis, I fixed the group size as 12. A certain arbitrariness of this value can be argued, because by manipulating with the group size one could increase the significance artificially. However, some choice is needed for the technique used; the actual one was fixed at the initial stage of the study and was never modified later. The same "manipulation" argument can be applied to the choice of the beginning of the first group. It was always fixed at the

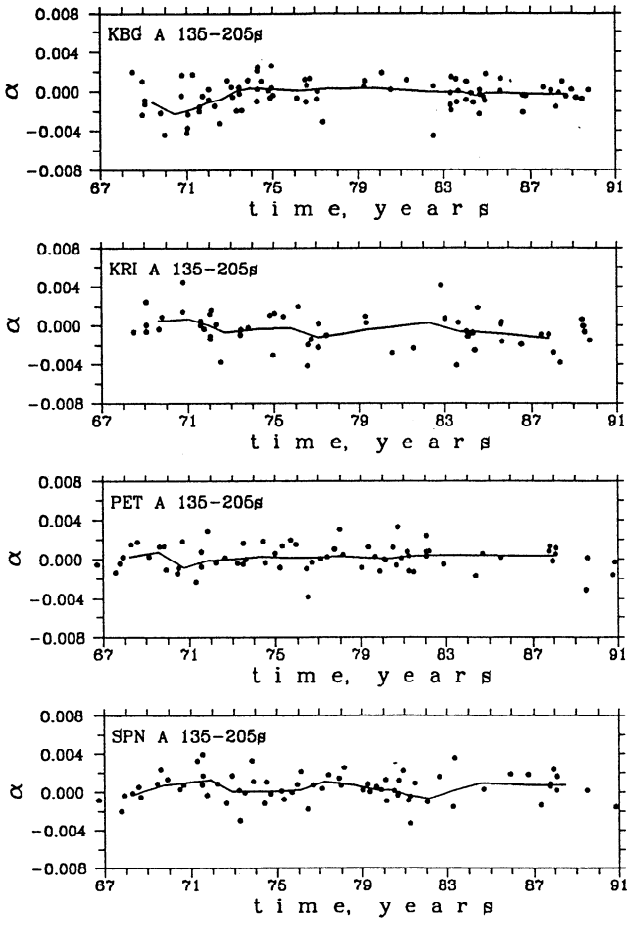

Figure 8. Individual uncorrected α values for the 135- to 205-s window versus event time for four stations, averaged over three components. The lines connect medians of successive eight-point groups.

earliest point in a data set, and the last incomplete group was excluded from the analysis.

The results of this test, performed for each station and component, are listed in Table 1, for the corrected data sets. Each line of Table 1 corresponds to a data sequence consisting of N successive points. A sequence is divided into $m+1$ successive equally sized 12-point data samples; then two variance estimates are found, representing within-group and intergroup variation, and their ratio (that is, F value) is calculated. At the null hypothesis: "within any group, the mean value is the same, common for all groups", both variances are, on the average, equal. To judge the significance of a deviation from the null hypothesis, one can compare the F value calculated from data (column F) with the theoretical 99% or 99.9% quantile of the F distribution with m and n degrees of freedom (where $n=N-m-1$), denoted $F_{m,n,99\%}$ and $F_{m,n,99.9\%}$. When the null hypothesis is valid, the situation "$F>F_{m,n,Q\%}$" arises in 100-Q% of cases, and the observed realization of this inequality means a significant (at 100-Q% level) deviation from the null hypothesis. Such cases are marked in Table 1; in these cases, the 12-event group averages are not all equal to some common constant, that is, a significant temporal variation is present. One can see that for the 45- to 135-s window, a significant (at 0.1% level) variation is found in four out of the eight cases studied.

The described ANOVA analysis has been applied to the Z and H components of the four stations that may be considered as independent, individual data sources. I can construct now a combined statistical measure of significance based on the whole data set. To do this, I can employ the fact that I have found, for each data sequence analyzed, the significance level, i.e., the probability to obtain the same result in the case of the null hypothesis. Assume that this probability is below some p for i out of k independent sources. Actually, $p=0.001$ (=100%-99.9%), $k=8$ and $i=4$. In order to determine the significance value for this observation one can treat it as a set of i successes in k standard Bernoulli trials with the probability p. Then the probability to obtain no less than i successes can be evaluated from the standard binomial distribution. This probability will specify the joint significance level sought. Reasoning in this way, for the case "$p=0.001$, $k=8$, and $i=4$," one obtains the probability value below 10^{-10}. Thus the presence of an apparent temporal variation for the 45- to 135-s window

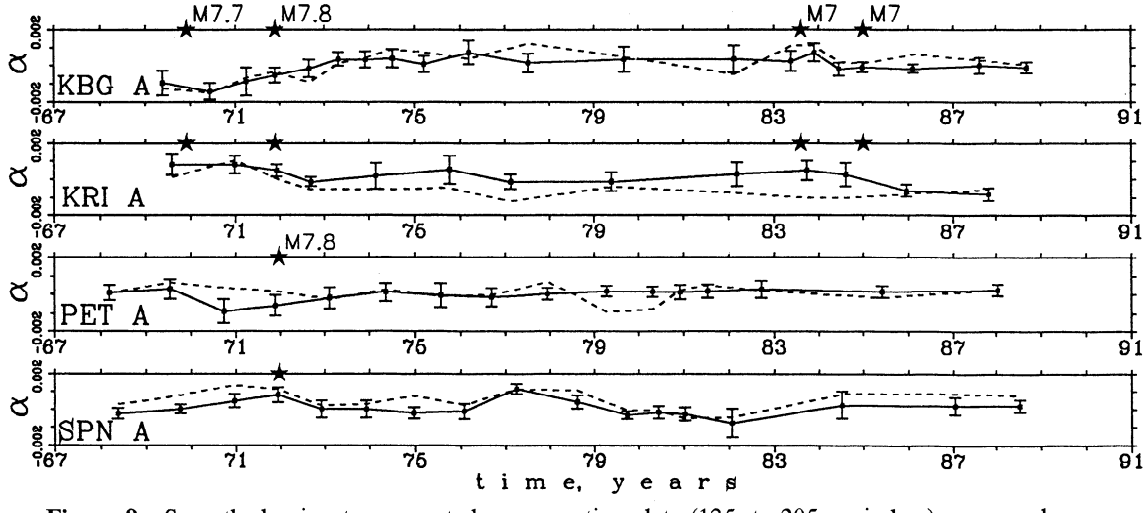

Figure 9. Smoothed epicenter-corrected α versus time data (135- to 205-s window), averaged over three components. Four graphs, one for each station, are shown. Other details are the same as for Figure 7.

data has the joint significance level below 10^{-10} and can be considered as proven. For the 135- to 205-s window, the corresponding set of parameters is "$p=0.01$, $k=8$, and $i=1$," giving the joint significance level of 8%. In this case, the presence of temporal variation can be suspected from the data but clearly cannot be considered as proven.

To avoid possible confusion, I must clarify the meaning of "independence" of input data sequences for various components and stations. They are independent in the sense that these sequences have no known intrinsic reason to coincide. At the same moment, these observations may well be dependent in the probabilistic sense. Furthermore, this kind of dependence is an additional argument in support of reality of the assumed temporal variation. Also, this kind of dependence in no sense contradicts treating the data sequence as independent data sources. In other words, each sequence can be thought of as a witness, and the fact that witnesses agree on some fact normally ought to be considered as an indication of high reliability of this fact and not as an argument against their reliability.

Still, an objection can be put forward, that some or all "witnesses" can be in common error because of some common biasing factor. It is practically impossible to answer the criticism of such a general kind. However, for a particular kind of common error, a relevant statistical check can usually be proposed. For example, one can imagine that the correlation between components of the same station is caused by unnoticed T phase arrivals produced by some specific epicenter location which occurred often during some particular time period (one such case was in fact revealed; see *Gusev and Lemzikov* [1980] for a map with a cluster of efficient T phase generating epicenters). To guarantee oneself against errors of this kind, one can confine the analysis by one component at each station. For example, using solely horizontal components, one obtains the case "$p=0.001$, $k=4$ and $i=3$" with the corresponding value of binomial probability below 10^{-8}, which is again very low.

One could try some more common technique of proving the reality of temporal variations, based on the Student t statistics. This approach is well illustrated by Figure 7 where group averages are shown with their "1σ" error brackets. One can see that the differences between average α values for many particular pairs of eight-point group averages on the same plot are in many cases obviously large in terms of "the number of sigmas," and a high significance for these differences can easily be shown by the Student test for any such pair. This visually transparent mode of reasoning is not quite convincing, however. One can easily object that there are so many pairs of eight-event groups that some of them must show a large, formally significant, difference, merely as a statistical fluctuation, without any real variation. It is in order to answer to the criticism of this kind that I used the more rigorous ANOVA approach. I consider it as an adequate one for my task: to show that α values follow the model "a nonconstant function of time + noise" rather than the zero hypothesis "a constant + noise."

Correlation Between Data Sequences and Possible Nodal Plane Variation Effects

Now I believe that the α fluctuations seen in Figure 7. are proven to be significant. This does not prove, however, that they represent true temporal variations. There is a serious unchecked source of fictitious variations, namely, nodal plane variations. Ideally, one would prefer to analyze data either with a fixed nodal plane orientation or with a fully random one; the first one would produce some spatially smooth bias that can be strongly suppressed by epicentral corrections of the kind described above, whereas the second one would produce uncorrelated random noise. Both cannot imitate temporal variations. To make this evident for the second case, assume for a moment that significant fluctuations of Figure 7 are produced by such a noise. Then if one would randomly shuffle the data points over the time axis, this would not alter the amplitude of fluctuations. It is easy to show that this prediction is incorrect: after actually performing such a shuffling, one obtains low F values that agree with the null hypothesis of the lacking temporal variation.

However, in the practical case of unknown and arbitrary nodal plane orientations one cannot exclude their systematic variation in time. I have not at hand any statistical procedure that could isolate or suppress apparent variations of such a kind. However, I can employ a technique that shows that the nodal-plane-related cause of anomalies is unlikely. Note that because of the wide sector of source back-azimuths at each station, combined with a considerable depth range, nodal planes must rotate in a rather specific, coordinated manner to produce an anomaly on a single station. Though this can be imagined for any particular station, it is highly improbable for two stations whose azimuths are different by as much as, typically, 90° or more, to show positively correlated anomalies produced in such a manner. By virtue of reciprocity, this is true also for a single station and two epicentral regions. Therefore if these two types of correlation are present, this will be a substantial argument against the nodal-plane-related cause of the variations. Checks of both described types have been made.

To perform such checks, the data were averaged again, now over 1-year intervals (at difference with constant-size groups used before). This allows one to study correlation between the time series of yearly averages. A value of correlation coefficient ρ was calculated for each analyzed pair of 24-point time series. One can then test the reality of correlation, i. e., the significance of a (positive) deviation of ρ from zero, using the standard technique based on the Student t statistic. Actually, because of gaps in the data, only 22 pairs of 1-year averages could be used for the KBG-KRI pair. In Table 2, I give the interstation ρ values and the t values to check the hypothesis $\rho > 0$. (This type of the null hypothesis is used because both numerically small or large negative values of correlation coefficient must be considered

Table 2. Correlation Coefficients Between Yearly Averages of α Values (45- to 135-s Window) of Station Pairs and their Significance Checked by the Student t Test

Station 1-Station 2, and Component	N	ρ	t	$t_{theo,95\%}(N\text{-}2)$
KBG-KRI Z	22	0.344	1.90	1.72
KBG-KRI H	22	0.122	0.58	1.72
PET-SPN Z	24	0.402	2.44	1.72
PET-SPN H	24	0.451	2.85	1.72

as not supporting my assumptions.) To calculate the observed t values, I use [*Press et. al.*, 1986]

$$t=\rho[(N-2)/(1-\rho^2)]^{1/2}. \quad (3)$$

These values can be compared with the theoretical 95% quantile $t_{theo}(n, 95\%)$ of the Student distribution with $n=N-2=20-22$ degrees of freedom. In three out of the four independent checks, the calculated t value is above the theoretical one; thus the correlation is significant at the 5% level. To obtain the joint significance level for all four cases studied treated as a whole, one can use again the binomial law in a way described above with respect to the F values. For the parameter combination "$p=0.05$, $k=4$, $i=3$," one obtains the probability of about 5×10^{-4}. This number gives the joint significance level sought. Thus the check is positive. Note in addition that in spite of the low significance of the ANOVA test for PET (Table 1), the correlation between SPN and PET is significant at the 5% level for the H component, and this suggests that temporal variation is present the station PET as well.

In Table 3, I show the results of the same type of analysis when the data sets of each station were divided into two equally sized subsets based on epicenter location. For each of four stations, two independent tests of this kind have been performed, using either the value of latitude or longitude to separate the data into two independent subsets. In each test the data of each subset were converted into the time series of yearly averages, and the correlation between these series gave the ρ value. In four out of the eight cases listed, the t test gives the significance levels below 1%; this yields the joint significance level below 10^{-6}. (Only the results for the H component are given; those for the Z component are similar.) Note that the results for two series of tests based on the interstation correlation and on the correlation between epicentral groups are independent. Taken as a whole, these results can be considered as a sufficiently strong argument against the idea that the observed temporal anomalies are only apparent and are actually produced by a coordinated nodal plane variation. All the discussion on the nodal-plane-related variations can be repeated literally with respect to the spurious effects of variable source directivity.

All the evidence discussed in this and the preceding sections, regarding various possible causes of apparent temporal anomalies and their qualification for the data set under study, is summarized in Table 4. The conclusion of this discussion is that none of these causes can explain the whole set of observations, so that the variations seen in Figure 7 can be considered as mostly genuine. Furthermore, some of the excursions appear to be of a precursory value, a point discussed in the next section.

Table 3. Correlation Coefficients Between Yearly Averages of α Values (45- to 135-s Window) for Pairs of Spatially Divided Subsets of Data of the Same Station (H Component Only) and their Significance Checked by the Student t Test

Station	Latitude or Longitude	Threshold Value	N	ρ	t	$t_{theo,99\%}$
KBG	λ	163.7°E	21	0.49	2.99	2.54
	ϕ	55.5°N	21	0.57	3.85	2.54
KRI	λ	162.3°E	22	0.28	1.50	2.53
	ϕ	55.0°N	23	0.16	0.84	2.52
PET	λ	159.9°E	22	-0.20	-0.80	2.53
	ϕ	52.6°N	23	-0.26	-1.04	2.52
SPN	λ	160.0°E	21	0.70	5.57	2.54
	ϕ	52.6°N	23	0.65	4.98	2.52

Table 4. Summary of Investigation of Possible Causes of Apparent Temporal Variations of the Coda Decay Rate

Cause	Qualification and Its Basis
1. Random, nonsignificant fluctuations	**no**: variations are significant
2. Mimicking by epicentral variation, e.g., related to T phases or trapped low-velocity waves	**unlikely**: when the epicenter-related variations had been compensated for, temporal variations persisted
3. Mimicking by depth variation	**no**: depth dependence is weak, depth-time correlation is absent
4. Mimicking by magnitude variation	**no**: magnitude dependence is weak, magnitude-time correlation is absent
5. Mimicking by nodal plane or source directivity variation	**unlikely:** variations correlate between stations and epicentral regions, over wide azimuthal sectors
6. Mimicking by variation of source spectra	**unlikely:** in the only clear case of such variation, anticipated and observed effects are of opposite sign
7. Effect of coda Q versus lapse time dependence	**no:** fully excluded both by the α technique and additionally by use of a fixed time window
8. Effect of oversampling in swarms	**no:** swarms were intentionally decimated
9. Calibration/instrument problems	**unlikely:** magnification error irrelevant, pendulum period shift not observed or of negligible effect
10. Human error	**unlikely:** no expressed anomalies in 135- to 205-s window as compared to 45- to 135-s window, despite identical measurement procedures

Precursory α Anomalies: Retroactive Study and Real-Time Monitoring and Analysis

Now I discuss the precursory interpretation of temporal variations, beginning with the probable precursors of $M=7.5$-8 earthquakes. In Figure 10, I compare the epicenter-corrected $\alpha(t)$ plots (45- to 135-s window) between stations. Information on large earthquakes (see Figure 1) is also added. One can see that for the KBG-KRI pair, a conspicuous negative anomaly is present in 1971, preceding the December 15, 1971, $M_{LH}=7.8$ earthquake located in the vicinity of both stations. This anomaly, detected by the earlier version of the technique used here, was the first coda precursor to be reported [*Gusev and Lemzikov*, 1980]. A similar anomaly is seen for KBG in 1969, except that its detection is somewhat less reliable as it arose in the beginning of the observation period. It precedes the November 22, 1969, $M_{LH}=7.7$, M(tsunami)≈ 7.8 earthquake

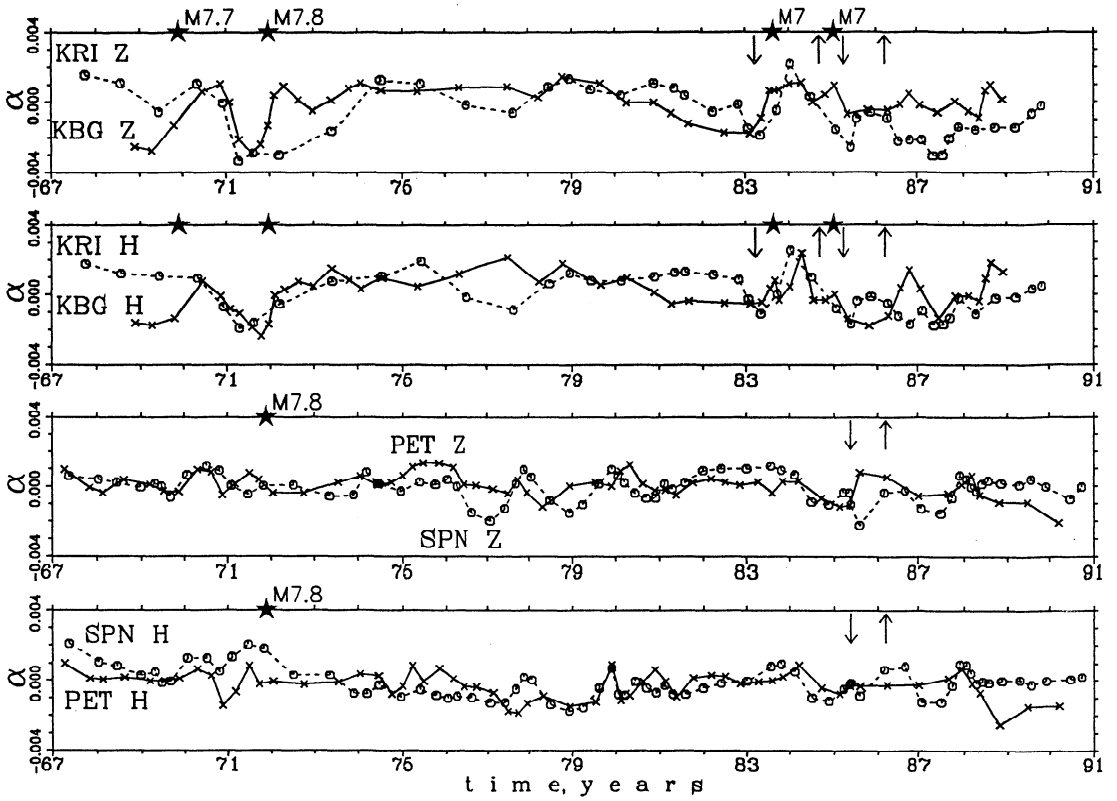

Figure 10. Comparison of $\alpha(t)$ graphs (epicenter corrected, 45- to 135-s window) between stations (in pairs). Arrows indicate the history of the real-time prediction experiment. A down arrow denotes an announcement and an up arrow denotes a cancellation of a real-time alarm for large (M=7.5-8) events in the vicinity of each station pair.

located to the north of KBG and far from KRI (see Figure 1). A much smaller baylike positive anomaly is present at PET before the November 24, 1971, M_w=7.6, h=100 km event located near PET, practically under the station SPN. In Figure 9 one can also see a long-term anomaly on the plot for KBG (135- to 205-s window) in 1969-1971. This anomaly began in advance of both earthquakes that occurred in the vicinity of this station. No other earthquakes with M_w>7.0 occurred on or around Kamchatka during the period of study. (The M=7.6 event of February 28, 1973, occurred near the southernmost promontory of Kamchatka, far from both station pairs discussed here).

As the existence of temporal variations in general is already proven, I check now only the statistical significance of individual conspicuous baylike features chosen by eye. (The present signal-to-noise ratio as well as the limited data volume unfortunately preclude a more strict approach, like the one employed by *Gusev* [1995a].) To do this, I specify, for each presumed anomaly, the "anomalous" period and the corresponding reference/"normal" period and then show that the average α values are significantly different between these two periods (see Table 5). In principle, one would prefer to use the reference period that precedes any anomaly, because the period after an anomaly may be contaminated by coseismic effects. However, this cannot be done for KBG because of overlapping anomalies and insufficient history. Also, it was reasonable to use the common reference period for both stations of a pair. Thus I specified the reference period for KBG and KRI as the whole period after the 1971 event. For PET I use the preanomaly period. The two average α values for the two periods were compared by the common two-sample Student t test. The results are given in Table 5 for three-component average α values. One can see that all listed (negative)

Table 5. Check of Significance of Individual, Averaged Over Three Components, Precursor-like α Anomalies, Associated With M=7.6-7.9 Earthquakes

Station	AI[a]	RI[b]	N_a	N_r	σ[c]	$\delta\alpha$[d]	t_{calc}[e]	$t_{theo,95\%}$[f]
			45- to 135-s Window					
KBG	70.96-71.96	71.96-92.0	20	172	1.9	-1.4	-3.14	1.98
KRI	70.96-71.96	71.96-92.0	12	150	1.9	-1.6	-2.84	1.98
KBG	68.9-69.9	71.96-92.0	9	172	1.9	-2.7	-4.09	1.98
PET	70.6-71.6	66.8-70.6	15	41	1.6	-1.0	-2.06	2.00
			135- to 205-s Window					
KBG	67.0-71.96	71.96-92.0	16	69	1.4	-0.9	-2.26	1.99

[a]Time interval of the presumed anomaly, contains N_a points.
[b]Reference time interval, contains N_r points.
[c]Sample standard deviation of α, calculated from both intervals combined, in 10^{-3} s^{-1} units.
[d]Estimated α difference (anomaly minus reference), same units.
[e]Value of the Student t statistic calculated from the data.
[f]Critical 95% value of the theoretical t distribution, to be compared with t_{calc}.

anomalies produce numerically large negative t values, which are significant at the 5% level. This is a strong argument against a purely random cause of the anomalies, and one can consider them as probable examples of genuine precursors. Unfortunately, this qualification cannot be checked in any strict way with the data volumes and time intervals of the size used here (or comparable): they cover no more than a small part of the interevent period for large earthquakes, and only two particular locations along a seismic belt.

Along with assumedly precursory excursions, on the same plots one can see nonprecursory anomalies of a comparable amplitude. Thus, while the precursory meaning of the listed particular anomalies seems probable, the general association between anomalies and imminent M=7.5-8 earthquakes cannot be justified. If used for the real prediction of such earthquakes, the α anomalies would produce a significant number of false alarms.

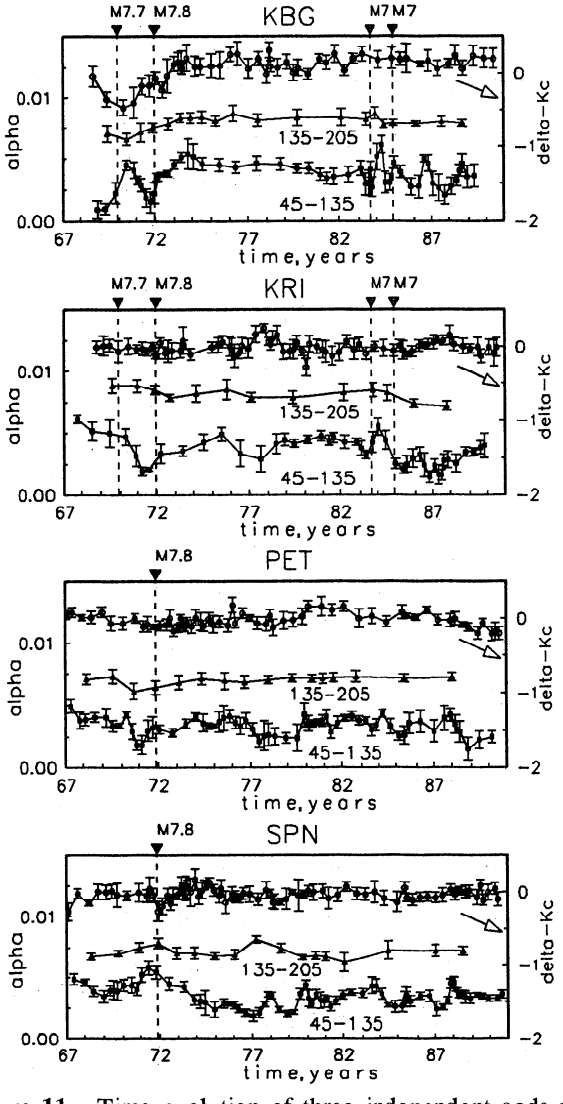

Figure 11. Time evolution of three independent coda parameters: relative coda level anomaly ΔK_C [*Gusev*, 1995a] (right scale) and two variants of the coda decay rate - α(135-205 s) and α(45-135 s) (left scale). For each parameter, averages over three components of a station are given, for successive 12- or 8-point groups. Error bars are $+1\sigma$ for group averages. Note the coincidence of anomalies for ΔK_C and α(135-205 s) in 1969-1971 and generally higher stability of ΔK_C compared to α(45-135 s).

This conclusion agrees with the results of the real-time prediction experiment carried out in 1982-1990 based on α anomalies. Soon after the beginning of this experiment in 1982, a moderate negative α anomaly was detected at the KBG-KRI station pair. An official prediction statement was issued in February 1983 specifying the magnitude range as 7.5-8, the region as the one adjacent to the stations, and the time window as the next halfyear. In June, the revised prediction statement was issued; it confirmed the previous magnitude and location forecast, and the most probable time window was specified as July-September 1983. A M_w=7.0 event occurred on August 17, 1983, within the predicted area, at depth h=85km (see Figure 1 for location). The alarm was continued further and was revoked in June 1984. On December 28, 1984, another moderate-to-large event took place in the prediction area, with M_w=6.7 and M_{LH}=7.5, not anticipated by a formal forecast. New negative α anomalies were detected in 1985, and alarms (for the same magnitude range) were issued in spring 1985 up to February 1986 in both zones studied (KBG-KRI and PET-SPN). No significant earthquakes occurred, and no more alarms were issued in 1985-1990. Alarm periods are indicated by arrows in Figure 10. The data analysis procedures employed in the real-time processing were comparable to ones used here, and one can see on Fig.10 the negative excursions that were considered as a basis for issuing successful and false alarms.

Recently, I studied the relative coda level, i.e., station coda amplitude residual, with the average coda amplitude over a network [*Gusev*, 1995a] as a reference. In that study, significant precursory anomalies were revealed, with no evidence of false alarms. In Figure 11, I compare the results of that and the present technique for the four stations studied here. One can see that the relative coda level shows only one clear anomaly, at KBG, and that this anomaly is well correlated with the anomaly of α (135-205 s) at the same station. The typical measurement time for the relative coda level data is around 135 s, so that both these parameters are associated, roughly, with the same coda segment. This correlation gives additional support to the reality of precursory α anomalies.

Discussion

General earthquake prediction issues, with respect to any potentially informative parameter, e.g., the coda decay rate, can be formulated as a four-stage sequence:

1. Do genuine temporal variations of the parameter exist?

2. If yes, (1) are they related to large earthquakes in general, and (1) do they come in advance of them? Or can one show that a forecasting procedure can be formulated retroactively, whose efficiency is significantly better than a blind try?

3. If yes, are the precursors detectable and usable in practice? Or can one implement a real-time version of the above forecasting procedure?

4. If yes, can one attain such combination of the values of the forecasting efficiency (defined below) and of the relative summary alarm dutation, that the forecasting procedure (now worthy of being named a technology) is socially valuable?

I would like to emphasize the difference of statistical evidence needed to claim 2 or 3 on the one hand or 4 on the other. This difference can be expressed numerically in terms of "forecasting efficiency," defined by *Gusev* [1974] as a ratio of the event rate over time intervals (more accurate, space-time volumes) of forecast to its a priori/average value (equivalent to the "probability gain" of *Aki* [1981]). In 2 and 3, the forecasting efficiency must be significantly different from unity (and may be equal to, say, 1.2), and this fact may be of great scientific value; whereas in 4, it must be large as compared to unity, (say, no less than 4). (Both figures above assume some reasonable fixed level of the relative summary alarm duration.)

If seen in such a technological perspective, the described results of the retroactive data analysis are not very promising, as they show prominent nonprecursory variations. Nor does the experience of the real-time prediction raise large hopes: it can be qualified as a limited success in scientific terms, but it cannot be considered as an impressive demonstration of prediction technology. In general, the presented Kamchatkan evidence suggests the following answers to the questions listed above: question 1, yes; question 2, probably yes; question 3, possibly yes, but with a significant false alarm rate; and question 4, definitely no. Although the situation may improve somewhat with larger data volumes and better data quality, nonprecursory temporal variations of the coda decay rate [*Jin and Aki*, 1989, 1992] seem to be a typical phenomenon, making the reliable identification of precursory anomalies on their background a difficult task.

This pessimistic view is specific, however, with respect to the coda decay rate proper. Other more successful data analysis techniques can be designed employing the same general idea of monitoring coda properties. For example, the relative coda level [*Gusev*, 1995a] demonstrates much better "signal-to-noise ratio," with a significance level of the order of 0.1% for continuous coda variations and of the order of 10^{-8} for baylike precursory variations, all this for manually measured unfiltered analog data. Another promising line of improvement is the application of better theoretical coda formation models as a basis for data analysis and the use of digital recording.

Let us consider now the possible mechanisms of the decay rate variation. In earlier work [*Gusev and Lemzikov*, 1980, 1984, 1985; *Aki*, 1985], the α variations were believed to be caused by changes of intrinsic loss change in the lithosphere. However, this model was incapable of explaining some specific coda envelope shape peculiarities, namely, humps superposed on a relatively smooth decay. These humps were interpreted as the manifestation of local time-dependent variations of the scatterer density [*Gusev and Lemzikov*, 1984; 1985]. The recent analysis of coda Q observations [*Gusev*, 1995b] showed that the role of intrinsic Q in the formation of coda shape at the lapse times in question (below 250 s) is probably negligible or at best secondary. This means that the earlier explanation of α variations through the intrinsic loss change is incorrect, and the most likely cause of the coda shape variation, including both the variation of the decay rate and the mentioned humplike features, is the temporal variation of the scatterer density. These assumed variations of the scatterer density are necessarily local: a synchronous relative change of the scatterer density over a large region and over all depths would leave coda shapes unaffected (only the absolute coda level would change). Impressive evidence of highly nonuniform spatial distribution of the scatterer density on a somewhat smaller distance scale has recently been presented by *Aptikaeva and Kopnichev* [1993].

The change of physical interpretation described above does not affect the validity of the earlier observational results of *Gusev and Lemzikov* [1980, 1984, 1985]. (They include three more examples of significant precursory anomalies in addition to the five ones shown here.) Also, the older data need not be revised in view of the new evidence on the spatial variations of α because systematic checks of epicentral wandering were performed, as explained above.

The new interpretation of temporal variations of α sheds new light onto the old result of A. A. Gusev and V. K. Lemzikov (limited-circulation report, 1984), who studied a few band-filtered codas of stations KBG and KRI for 1970-1971 and found that the temporal α variation is expressed in the 0.5-to 2-Hz frequency range only and disappears for the 4- to 8-Hz range. This result had no rational explanation in terms of the intrinsic loss concept but poses no serious problem within the scatterer-density context. It suffices to assume that additional scatterers are of a large size, so that they interact only weakly with higher-frequency waves. Such an assumption evidently is remniscent of the ideas of *Jin and Aki* [1989, 1992] on the existence of characteristic structural sizes in the lithosphere.

Another conclusion of *Gusev* [1995b] is the localization of most coda-producing scatterers near the Earth's surface. This type of the scatterer distribution is qualitatively different from the constant-density distribution of *Aki and Chouet* [1985]. Note that in terms of the single isotropic scattering model used by *Gusev* [1995b], the coda level is determined, at any given moment, by the number of scatterers within a narrow ring, and not within a half sphere as in the work of *Aki and Chouet* [1985], so that the effect of a particular fluctuation of the scatterer density is much more pronounced in the first case. This may be true with respect to both temporal and spatial variations. However, in order to explain the variations seen in Figure 6, one needs to consider the three-dimensional picture. In the case of station KRI, where the spatial variation is the most expressed, the average α pattern shows a clear increase of absolute α values from the continent to the ocean. The steeper coda decay for the sources nearer the trench may indicate faster depth decay of the scatterer density in the relatively homogeneous oceanic plate, as compared to the subduction zone proper.

Now let us assume that the presented interpretation of temporal variations of coda shape by time-varying scatterer density is correct and discuss physical processes that may cause such a variation. Unfortunately there is somewhat discouraging general background for such a discussion. In 1970-1985, many publications considered "physics of earthquake precursors," often limited to direct application of laboratory specimen fracture data to in situ Earth phenomena. Now many people see much of this "physics" as an expression of wishful thinking, and there are also wide doubts regarding mere reality of reported precursory phenomena. Despite such a background I shall give a short summary of probable characteristic features of the scatterer density variation. One evident feature is its large scale.

Using the single-scattering model and ascribing the α variation to coda lapse time of 80 s (the middle of the window used), one obtains the value of one-way (source-to-scatterer or scatterer-to-station) travel time of about 40 s and thus the station-to-scatterer distance of about 150 km. A change of α may indicate the change of the scatterer density at some distance range well below this value, say, at distances around 80 km. To produce a clear anomaly, a large part of scattering volume/layer, covering, say, 90° in terms of azimuth at a receiver station, must change its properties. Therefore the characteristic size of the anomalous zone may be of the order of 100 km or even larger. The change of scatterer density over such a considerable volume can be relatively abrupt, taking sometimes no more than 1-2 months (see Figures 4 and 7). The scarce data on the frequency dependence of anomalies cited above provide some inference on the typical size of the scatterers involved. Assuming the upper frequency boundary for the noticeable precursory variation of scatterer density to be equal to 3 Hz, one can roughly estimate the size of a typical time-varying scatterer as 1 km or larger. The described properties of the observed variations (the scale, the time constant, and the scatterer size) provide the important constraints for an acceptable physical model of variations of the scatterer density. Another important property, the one specific for precursory anomalies, is the negative sign of an anomaly; this probably indicates that the scatterer density increases in the anomalous zone described above.

All these constraints do not immediately suggest any particular physical explanation, neither for the variation in general, nor for precursory anomalies. There exists, however, a seemingly applicable idea, mentioned by V. I. Keilis-Borok, of a pulselike fluid injection from the mantle. Such an injection may increase the pore pressure and open/widen the rock joints at depth over a considerable area. This may cause two effects: an immediate increase of the scatterer density over the area producing an observable α precursor and also an increase of the large earthquake probability over a considerable time period, say, 1-2 years. Despite its rather speculative character, this idea agrees with all constraints and thus deserves some attention. All the above considerations are very preliminary: the data volume and quality preclude any deep analysis.

Summarizing this discussion, one can believe that the interpretation of spatial and temporal variations of coda shapes in terms of the varying scatterer density may provide new types of information on temporal variations of lithospheric properties, including possible precursors.

Conclusions

1. The data on the small event coda decay rate for 24 years of observation for two pairs of stations suggest clear apparent temporal variation for the lapse time window of 45-135 s.

2. Several causes of possible mimicking of temporal variation by changes of other parameters are investigated; the most important is the spacial variation of coda shape. The conclusion of this investigation is that the temporal variation is probably genuine.

3. Retroactive and real-time identification of precursory coda decay rate variations has been carried out. Five cases of conspicuous precursor-looking anomalies are found. Each of the five anomalies is statistically significant. Data are insufficient for statistically grounded association of apparent precursors with large earthquakes.

4. Real-time monitoring and detection of precursory anomalies has been performed during a 9-year period; it yielded a successful prediction and a false alarm.

5. The older physical interpretation of the coda shape variations through the variation of intrinsic loss is rejected. Spatial and temporal variations of the local scatterer density is considered as a probable cause of spatial and temporal variations of coda shape.

Acknowledgments. The author is indebted to the administration of the Institute of Volcanology and Kamchatkan Experimental-Methodical Seismological Party for providing access to the archive of seismograms. Data processing was mostly supervised by Vladimir Lemzikov; he also participated (1981-1986) in the real-time data analysis. Financial support by the Russian Foundation for Basic Research, (RFFI grant 93-05-8514) is gratefully acknowledged. I am indebted to S. Hough, Associate Editor, to M. Hedlin, referee, and to the anonymous referee for comments and valuable suggestions that improved the paper.

References

Aki, K., Analysis of the seismic coda of local earthquakes as scattered waves, *J. Geophys. Res., 74*, 147-156, 1969.

Aki, K. A probabilistic synthesis of precursory phenomena, in *Earthquake Prediction: An International Review, Maurice Ewing Ser.*, vol. 4, edited by D.W. Simpson and P.G. Richards, pp. 566-574, AGU, Washington D.C., 1981.

Aki, K., Theory of earthquake prediction with special references to monitoring of the quality factor of lithosphere by coda method, *Earthquake Predict. Res., 3*, 219-230, 1985.

Aki, K., and B. Chouet, Origin of coda waves: source, attenuation and scattering effects, *J. Geophys. Res., 80*, 3322-3342, 1975.

Aptikaeva, O. I., and Yu. F. Kopnichev, Space-time variations of the coda wave envelopes of local earthquakes in the region of Central Asia. *J. Earthquake Predict. Res., 2,* 497-514, 1993.

Beroza, G., A.T. Cole, and W.L. Ellsworth. Stability of coda attenuation during the Loma Prieta, California, earthquake sequence. *J. Geophys. Res. 100,* 3977-3987, 1995.

Chouet, B., Temporal variation in the attenuation of earthquake coda near Stone Canyon, California, *Geophys. Res. Lett., 6,* 143-146, 1979.

Got, J. L., and J. Frechet, Origin of amplitude variations in seismic doublets: Source or attenuation process?, *Geophys. J. Int., 114,* 325-340, 1993.

Got, J. L., G. Poupinet, and J. Frechet, Changes in source and site effects compared to coda Q^{-1} temporal variations using microearthquake doublets in California, *Pure Appl.Geophys., 134,* 195-228, 1990.

Gusev A. A., Earthquake prediction based on statistics of seismicity, in: *Seismicity, Seismic Prognosis, Upper Mantle Properties and Their Relation to Volcanism on Kamchatka* (in Russian), pp,109-119 Nauka, Novosibirsk, Russia, 1974.

Gusev, A. A. Baylike and continuous variations of the relative coda amplitude level during 24 years of observations on Kamchatka, *J. Geophys. Res., 100, 20311-20319,* 1995a.

Gusev, A.A., Vertical profile of turbidity and coda *Q, Geophys. J. Int., 123*, 665-672, 1995b.

Gusev, A. A., and V. K. Lemzikov, Preliminary results of the study of coda envelope shape variations of near earthquakes before the 1971 Ust-Kamchatsk earthquake (in Russian), *Vulkanol. Seismol., 6,* 82-93, 1980.

Gusev, A. A., and V. K. Lemzikov, Anomalies of coda wave parameters of small earthquakes before three large earthquakes of Kurile-Kamchatka zone (in Russian), *Vulkanol. Seismol., 4,* 76-90, 1984.

Gusev, A. A., and V. K. Lemzikov, Properties of scattered elastic

waves in the lithosphere of Kamchatka: parameters and temporal variations, *Tectonophysics, 112,* 137-153, 1985.

Hellweg, M., P. Spudich, J. B. Fletcher, and L. M. Backer, Stability of coda Q in the region of Parkfield, California: view from the U.S.Geological Survey Parkfield dense seismograph array, *J. Geophys. Res., 100,* 2089-2102, 1995.

Jin, A., and K. Aki, Temporal change in coda Q before the Tangshan earthquake of 1976 and the Haicheng earthquake of 1975, *J. Geophys. Res., 91,* 665-673, 1986.

Jin, A., and K. Aki, Spatial and temporal correlation between coda Q^{-1} and seismicity and its physical mechanism, *J. Geophys. Res., 94,* 14041-14059, 1989.

Jin, A., and K. Aki. Observational and physical bases for the coda Q^{1} precursor, in *Evaluation of Proposed Earthquake Precursors* edited by M. Wyss, pp. 33-46, AGU, Washington D.C., 1991.

Jin, A., and K. Aki, Temporal correlation between coda Q^{-1} and seismicity - Evidence for a structural unit in the brittle-ductile transition zone, *J. Geodyn., 17,* 95-120, 1993.

Lemzikov, V. K., and A. A. Gusev, Energy classification of near Kamchatka earthquakes using coda wave level (in Russian), *Vulkanol. Seismol., 4,* 83-97, 1989.

Press, W. H., B. P. Flannery, S. A. Teulkovsky, and W. T. Vettering, *Numerical Recipes,* Cambrige Univ. Press, New York, 1986.

Sato, H., Attenuation and envelope formation of three-component seismograms of small local earthquakes on randomly inhomogeneous lithosphere, *J. Geophys. Res., 89,* 1221-1241, 1984.

Sato, H., Temporal change in scattering and attenuation associated with the earthquake occurrence, *Pure Appl. Geophys., 126,* 2465-2497, 1988.

Wyss, M. (Ed.), *Evaluation of Proposed Earthquake Precursors,* AGU, Washington, D.C., 1991.

A. A. Gusev, Institute of Volcanic Geology and Geochemistry, Russian Academy of Science, 9 Piip Blvd., 683006 Petropavlovsk-Kamchatskii, Russia. (e-mail: seis@volgeo.kamchatka.su)

(Received August 18,1996; revised November 1, 1996; accepted November 6, 1996.)